alkali-metal and molybdenum oxide.

5. In situ heating of 6.4 wt % $Mo/SiO_2$ destroyed the polymolybdate clusters and led to the formation of a new $Mo^{6+}/SiO_2$ structure in which the $Mo^{6+}$ cations are isolated. The isolated $Mo^{6+}$ species reformed a polymolybdate cluster upon rehydration of the surface.

6. Previously reported UVDRS bands attributed to tetrahedrally coordinated Mo were observed, but the assignment to $Mo(T_d)$ is inconsistent with the LRS results which showed only $Mo(O_h)$ to be present.

*Acknowledgment.* This work was supported by the Robert A. Welch Foundation and the U.S. Department of Energy, Office of Basic Energy Sciences (C.C.W. and J.G.E), and by the Texaco Philanthropic Foundation (F.D.H.). We acknolwedge Prof. Y. Iwasawa for supplying one of the silica supports.

**Registry No.** Molybdenum oxide, 1313-27-5; calcium, 7440-70-2; sodium, 7440-23-5.

---

# A Raman and Ultraviolet Diffuse Reflectance Spectroscopic Investigation of Alumina-Supported Molybdenum Oxide

**Clark C. Williams,[†] John G. Ekerdt,[*]**

*Department of Chemical Engineering, University of Texas at Austin, Austin, Texas 78712*

**Jih-Mirn Jehng, Franklin D. Hardcastle,[‡] and Israel E. Wachs**

*Zettlemoyer Center for Surface Studies, Departments of Chemical Engineering and Chemistry, Lehigh University, Bethlehem, Pennsylvania 18015* *(Received: September 4, 1990; In Final Form: June 6, 1991)*

Laser Raman spectroscopy and ultraviolet–visible diffuse reflectance spectroscopy were used to characterize alumina-supported molybdenum oxide prepared from $Mo_2(\eta^3\text{-}C_3H_5)_4$, $H_2(MoO_3C_2O_4)\cdot 2H_2O$, and $(NH_4)_6Mo_7O_{24}\cdot 4H_2O$ at loadings ranging from 0.67 to 13.3 wt % Mo. The structure of the calcined $Mo^{6+}/Al_2O_3$, under ambient conditions, was found to be independent of the molybdenum precursor and the preparation pH. The hydrated surface molybdate structure was found to be governed by the inherent acid–base properties of the molybdena/alumina system and the molybdenum weight loading. At low Mo loadings (<1 Mo atom/nm$^2$), isolated $MoO_4$ tetrahedra dominate although a low degree of polymerization was observed. At 2–2.5 Mo atoms/nm$^2$, the majority of the molybdenum was incorporated into octahedrally coordinated molybdenum polyanions. Crystalline $MoO_3$ was detected above monolayer coverage (5–6 Mo atoms/nm$^2$).

## Introduction

Conventional impregnation of alumina with aqueous molybdate salts has been claimed to result in catalysts with nonuniform dispersion and coordination.[1] Organometallic compounds, $Mo(\eta^3\text{-}C_3H_5)_4$ and $Mo_2(\eta^3\text{-}C_3H_5)_4$, as well as organic and inorganic salts, $H_2(MoO_3C_2O_4)\cdot 2H_2O$ and $(NH_4)_6Mo_7O_{24}\cdot 4H_2O$ (AHM), have recently been used under controlled conditions in an attempt to prepare highly dispersed and uniformly coordinated molybdenum oxide surface species on alumina. Iwasawa and co-workers have examined $Mo/Al_2O_3$ catalysts prepared from $Mo(\eta^3\text{-}C_3H_5)_4$ and $Mo_2(\eta^3\text{-}C_3H_5)_4$ with X-ray photoelectron spectroscopy (XPS), ultraviolet–visible diffuse reflectance spectroscopy (UVDRS), laser Raman spectroscopy (LRS), extended X-ray absorption fine structure (EXAFS), stoichiometric ligand removal, and hydrogen and oxygen uptake.[2-4] The Raman spectrum of $Mo(\eta^3\text{-}C_3H_5)_4$-derived $Mo^{6+}/Al_2O_3$ displayed a Mo–O stretching band at 968 cm$^{-1}$ which was attributed to tetrahedrally coordinated $Mo^{6+}$. The $Mo^{6+}/Al_2O_3$ sample prepared from AHM displayed a Mo–O stretching band near 960 cm$^{-1}$ and was assigned to a pseudo-$MoO_6$ octahedral group.[2] They proposed that allylic precursors, after appropriate treatment, led to thermally stable, isolated or paired bidentate $MoO_4$ tetrahedra or tetrahedral dimers joined by bridging oxygen, depending on the alumina support and precursor. It was reported that the molybdenum in these compounds was uniformly coordinated and highly dispersed whereas in conventional catalysts, prepared from aqueous molybdenum salts, the molybdenum coordination number and degree of aggregation were variable.[4] Rodrigo et al.,[5-7] in contrast, obtained nearly identical XPS, secondary ion mass spectroscopy (SIMS), and UVDRS results for catalysts prepared from AHM and $Mo(\eta^3\text{-}C_3H_5)_4$. Although $Mo(\eta^3\text{-}C_3H_5)_4$-derived samples at low weight loadings were more active in low-temperature oxygen chemisorption than impregnated samples, it was concluded from UVDRS data that these oxygen-consuming species were not isolated $MoO_4$ tetrahedra.

Wang and Hall developed a method to adsorb $MoO_4^{2-}$ ions onto the alumina surface by maintaining the impregnation solution at pH 8–10.[8,9] They concluded from LRS and UVDRS that molybdate anions adsorbed under these conditions remained isolated during drying and calcination, whereas conventional pore filling with the heptamolybdate anions present at lower pH values led to polymeric molybdate species. Kasztelan et al.,[10] using a similar approach, have found that only 5% of the molybdenum adsorbed at low pH was removed by water washing after impregnation, whereas all of the molybdenum adsorbed at high pH could be removed, suggesting a limited interaction between $MoO_4^{2-}$ anions and the negatively charged surface, which was above its

---

[*] To whom correspondence should be addressed.

[†] Current address: Union Carbide Corporation, P.O. Box 8361, South Charleston, WV 25303.

[‡] Current address: Sandia National Laboratory, Division 1845, Albuquerque, NM 87185.

(1) Massoth, F. E. *Adv. Catal.* **1978**, *27*, 265.

(2) Iwasawa, Y.; Ogasawara, S. *J. Chem. Soc., Faraday Trans. 1* **1979**, *75*, 1465.

(3) Iwasawa, Y.; Sato, Y.; Kuroda, H. *J. Catal.* **1983**, *82*, 289.

(4) Iwasawa, Y. *Advances in Catalysis*; Academic Press: New York, 1987; Vol. 35, p 265.

(5) Rodrigo, L.; Marcinkowska, K.; Adnot, A.; Roberge, P. C.; Kaliaguine, S.; Stencel, J. M.; Makovsky, L. E.; Diehl, J. R. *J. Phys. Chem.* **1986**, *90*, 2690.

(6) Rodrigo, L.; Adnot, A.; Roberge, P. C.; Kaliaguine, S. *J. Catal.* **1987**, *105*, 175.

(7) Rodrigo, L.; Marcinkowska, K.; Lafrance, C. P.; Roberge, P. C.; Kaliaguine, S. *Proc. 9th Iberoam. Symp. Catal.* **1984**, 675.

(8) Wang, L.; Hall, W. K. *J. Catal.* **1980**, *66*, 251.

(9) Wang, L.; Hall, W. K. *J. Catal.* **1982**, *77*, 232.

(10) Kasztelan, S.; Grimblot, J.; Bonnelle, J. P.; Payen, E.; Toulhoat, H.; Jacquin, Y. *Appl. Catal.* **1983**, *7*, 91.

0022-3654/91/2095-8791$02.50/0

isoelectric point. Their Raman spectra demonstrated that molybdenum, which had adsorbed at pH values above the isoelectric point, polymerized during calcination. Other groups have also investigated the interaction of aqueous molybdenum species with $\gamma$-$Al_2O_3$ as a function of solution pH and loading and have characterized the species present before calcination.[11-15] At pH < 4 a polymeric species adsorbs while above pH 7 a monomeric molybdate predominates.

Ng et al.[16] studied the adsorption of molybdenum oxalate complexes on alumina with LRS and Fourier transform infrared spectroscopy (FTIR). The Raman $\nu$(Mo–O) frequency of $Mo/Al_2O_3$ samples prepared from $H_2(MoO_3C_2O_4)$ solutions and dried at 110 °C for 12 h was found to be pH dependent, leading them to conclude that dimeric molybdenum oxalate anions formed dimeric molybdate surface species upon adsorption at pH 2, whereas the monomeric anion, adsorbed at higher pH values, remained isolated. It was suggested that $H_2(MoO_3C_2O_4)\cdot 2H_2O$ may be a better candidate for catalyst preparation than AHM, which was shown to produce the same species upon drying, independent of initial pH. Tsigdinos et al., on the basis of adsorption stoichiometry, have also concluded that $H_2(MoO_3C_2O_4)$ can adsorb intact on alumina.[17]

LRS[2,8,18-35] and UVDRS[2,7,9,20,36-43] have been used extensively to characterize alumina-supported molybdenum oxide. Most of the above studies were done under ambient conditions. Several in situ studies have appeared that demonstrate the effects of hydration on the structure and bonding of molybdenum oxide on $Al_2O_3$.[27,30,33,34,44] In general, the molybdenum oxide species spread upon dehydration to form octahedrally coordinated $MoO_6$ units that are bonded to the support.[44] Different structures and Raman bands are formed if the surface is hydrated. The application of LRS to $Mo^{6+}/Al_2O_3$ prepared from $Mo_2(\eta^3$-$C_3H_5)_4$ has been limited to one sample;[2] most of the studies have used AHM to form $Mo^{6+}/Al_2O_3$. Raman spectra of $Mo/Al_2O_3$ prepared from $H_2(MoO_3C_2O_4)\cdot 2H_2O$ were reported only for uncalcined samples.[16]

This paper reports the structures formed when the surface molybdenum oxide species are hydrated. LRS and UVDRS are applied to calcined $Mo/Al_2O_3$ prepared from $Mo_2(\eta^3$-$C_3H_5)_4$, $H_2(MoO_3C_2O_4)\cdot 2H_2O$, and $(NH_4)_6Mo_7O_{24}\cdot 4H_2O$ to determine the effect of molybdenum precursor, preparation pH, and calcination temperature. The structure of molybdenum oxide supported on alumina, under ambient conditions, is shown to be independent of the preparation method as found for $Mo/SiO_2$[45] and $Mo/MgO$.[46] The key factor in determining the molecular structure of supported molybdena is the nature of the metal oxide support.

## Experimental Section

Molybdenum was supported on Harshaw (180 $m^2/g$) $\eta$-alumina and on Ketjen 000-1.5E (190 $m^2/g$) and Nishio (190 $m^2/g$) $\gamma$-aluminas. Nishio active alumina has been previously used to support $Mo_2(\eta^3$-$C_3H_5)_4$.[3]

$Mo_2(\eta^3$-$C_3H_5)_4$ was synthesized from the reaction between $C_3H_5MgBr$ and $Mo_2(CH_3CO_2)_4$, as described in a previous paper.[45] Alumina supports were calcined at 500 °C in dry air for 12 h, evacuated for 1 h, and then purged with argon for 1 h to remove adsorbed impurities, water, and excess hydroxyl groups. Addition of $Mo_2(\eta^3$-$C_3H_5)_4$ solutions and subsequent treatment steps were performed as previously reported.[45] Weight loadings obtained from allylic preparations ranged from 0.7 to 1.8% (expressed as percent Mo metal).

Temperature-programmed hydrogenolysis (TPH) was performed on $Mo_2(\eta^3$-$C_3H_5)_4$ anchored to Nishio alumina. After fixation and evacuation, samples were ramped from 25 to 575 °C over 2.5 h in 15 $cm^3$/min of 6% $H_2$ (balance $N_2$). Hydrocarbon products were analyzed with a Hewlett-Packard 5880A gas chromatograph equipped with a flame ionization detector and a Chrompack 50-m × 0.53-mm PLOT fused silica column.

A series of $Mo/Al_2O_3$ samples were prepared by using the equilibrium adsorption procedure developed by Wang and Hall.[9] Five-gram portions of Ketjen alumina were intermittently shaken in 250 mL of 0.007 M $(NH_4)_6Mo_7O_{24}$ (Alpha Products, 99.999%) for 18 h. After filtration, samples were dried at 130 °C for 6 h and then calcined at 500 °C for 3 h. Weight loadings increased from 0.5 to 2.0% Mo as initial pH decreased from 9.4 to 8.2. Final pH values of 9.6, 9.2, and 8.5 were measured for initial pH values of 9.4, 9.1, and 8.2, respectively.

Conventionally impregnated samples were also prepared from AHM and $H_2(MoO_3C_2O_4)\cdot 2H_2O$ (molybdenum oxalate). Pores of Ketjen alumina were filled with aqueous AHM, at the natural pH of 5–6 for the solution, dried at 120 °C for 14 h, and calcined at 500 °C for 3 h. Samples were prepared with 0.1–10% Mo. A series of AHM samples were also prepared on Harshaw alumina with loadings of 0.67, 2.0, 3.3, 4.7, 6.7, 10.0, and 13.3% Mo. These

---

(11) Mulcahy, F. M.; Fay, M. J.; Proctor, A.; Houalla, M.; Hercules, D. M. *J. Catal.* **1990**, *124*, 231.

(12) van Veen, J. A. R.; Hendriks, P. A. J. M. *Polyhedron* **1986**, *5*, 75.

(13) van Veen, J. A. R.; de Wit, H.; Emeis, C. A.; Hendriks, P. A. J. M. *J. Catal.* **1987**, *107*, 579.

(14) Mensch, C. T. J.; van Veen, J. A. R.; van Wingerden, B.; van Dijk, M. P. *J. Phys. Chem.* **1988**, *92*, 4961.

(15) van Veen, J. A. R.; Hendriks, P. A. J.; Romers, E. J. G. M.; Andrea, R. R. *J. Phys. Chem.* **1990**, *94*, 5275.

(16) Ng, K. Y. S.; Zhou, X.; Gulari, E. *J. Phys. Chem.* **1985**, *89*, 2477.

(17) Tsigdinos, G. A.; Chen, H. Y.; Streusand, B. J. *Ind. Eng. Chem. Prod. Res. Dev.* **1981**, *20*, 619.

(18) Brown, F. R.; Makovsky, L. E.; Rhee, K. H. *J. Catal.* **1977**, *50*, 162.

(19) Medema, J.; Van Stam, C.; De Beer, V. H. J.; Konings, A. J. A.; Koningsberger, D. C. *J. Catal.* **1978**, *53*, 386.

(20) Jeziorowski, H.; Knozinger, H. *J. Phys. Chem.* **1979**, *83*, 1166.

(21) Thomas, R.; Mittelmeijer-Hazeleger, M. C.; Kerkhof, F. P. J. M.; Moulijn, J. A.; Medema, J.; de Beer, V. H. J. In *Proceedings of the Climax 3rd International Conference on Chemistry and Uses of Molybdenum*; Climax Molybdenum Co.: Ann Arbor, MI, 1979; p 85.

(22) Cheng, C. P.; Schrader, G. L. *J. Catal.* **1979**, *60*, 276.

(23) Iannibello, A.; Marengo, S.; Trifiro, F.; Villa, P. L. In *Preparation of Catalysis II*; Delmon, B., Grange, P., Jacobs, P., Poncelot, G., Eds.; Elsevier: Amsterdam, 1979; p 65.

(24) Zingg, D. S.; Makovsky, L. E.; Tischer, R. E.; Brown, F. R.; Hercules, D. M. *J. Phys. Chem.* **1980**, *84*, 2898.

(25) Sombret, B.; Dhamelincourt, P.; Wallart, F.; Muller, A. C.; Bouquet, M.; Grosmangin, J. *J. Raman Spectrosc.* **1980**, *9*, 291.

(26) Lopez Agudo, A.; Gil, F. J.; Calleja, J. M.; Fernandez, V. *J. Raman Spectrosc.* **1981**, *11*, 454.

(27) Stencel, J. M.; Makovsky, L. E.; Sarkus, T. A.; de Vries, J.; Thomas, R.; Moulijn, J. A. *J. Catal.* **1984**, *90*, 314.

(28) Stencel, J. M.; Makovsky, L. E.; Diehl, J. R.; Sarkus, T. A. *J. Catal.* **1985**, *95*, 414.

(29) Makovsky, L. E.; Stencel, J. M.; Brown, F. R.; Tischer, R. E.; Pollack, S. S. *J. Catal.* **1984**, *89*, 334.

(30) Chan, S. S.; Wachs, I. E.; Murrell, L. L.; Wang, L.; Hall, W. K. *J. Phys. Chem.* **1984**, *88*, 5831.

(31) Dufresne, P.; Payen, E.; Grimblot, J.; Bonnelle, J. P. *J. Phys. Chem.* **1981**, *85*, 2344.

(32) Kasztelan, S.; Payen, E.; Toulhoat, H.; Grimblot, J.; Bonnelle, J. P. *Polyhedron* **1986**, *5*, 157.

(33) Payen, E.; Grimblot, J.; Kasztelan, S. *J. Phys. Chem.* **1987**, *91*, 6642.

(34) Payen, E.; Kasztelan, S.; Grimblot, J.; Bonnelle, J. P. *J. Raman Spectrosc.* **1986**, *17*, 233.

(35) Okamoto, Y.; Imanaka, T. *J. Phys. Chem.* **1988**, *92*, 7102.

(36) Ashley, J. H.; Mitchell, P. C. H. *J. Chem. Soc. A* **1968**, 2821.

(37) Ashley, J. H.; Mitchell, P. C. H. *J. Chem. Soc. A* **1969**, 2730.

(38) Asmolov, G. N.; Krylov, O. V. *Kinet. Katal.* **1970**, *11*, 1028.

(39) Asmolov, G. N.; Krylov, O. V. *Kinet. Katal.* **1972**, *13*, 188.

(40) Giordano, N.; Bart, J. C. J.; Vaghi, A.; Castellan, A., Martinotti, G. *J. Catal.* **1975**, *36*, 81.

(41) Che, M.; Figueras, F.; Forissier, M.; McAteer, J.; Perrin, M.; Portefaix, J. L.; Praliaud, H. In *Proceedings of the 6th International Congress on Catalysis, London, 1976*; The Chemical Society: London, 1977; Vol. 1, p 261.

(42) Praliaud, H. *J. Less-Common Met.* **1977**, *54*, 387.

(43) Iannibello, A.; Marengo, S.; Tittarelli, P.; Morelli, G.; Zecchina, A. *J. Chem. Soc., Faraday Trans. 1* **1984**, *80*, 2209.

(44) Hardcastle, F. D.; Turek, A. M.; Jeng, J.-M.; Vuurman, M. A.; Deo, G.; Wachs, I. E. Molecular Structures of Surface Metal Oxide Species by In Situ Raman Spectroscopy. *J. Phys. Chem.*, to be published.

(45) Williams, C. W.; Ekerdt, J. G.; Jehng, J. M.; Hardcastle, F. D.; Turek, A. M.; Wachs, I. E. *J. Phys. Chem.*, preceding paper in this issue.

(46) Williams, C. C.; Kohler, S. D.; Ekerdt, J. G.; Chen, C.-K.; Jehng, J.-M.; Hardcastle, F. D.; Wachs, I. E. Characterization of the Molybdenum Oxide Magnesia System. In preparation.

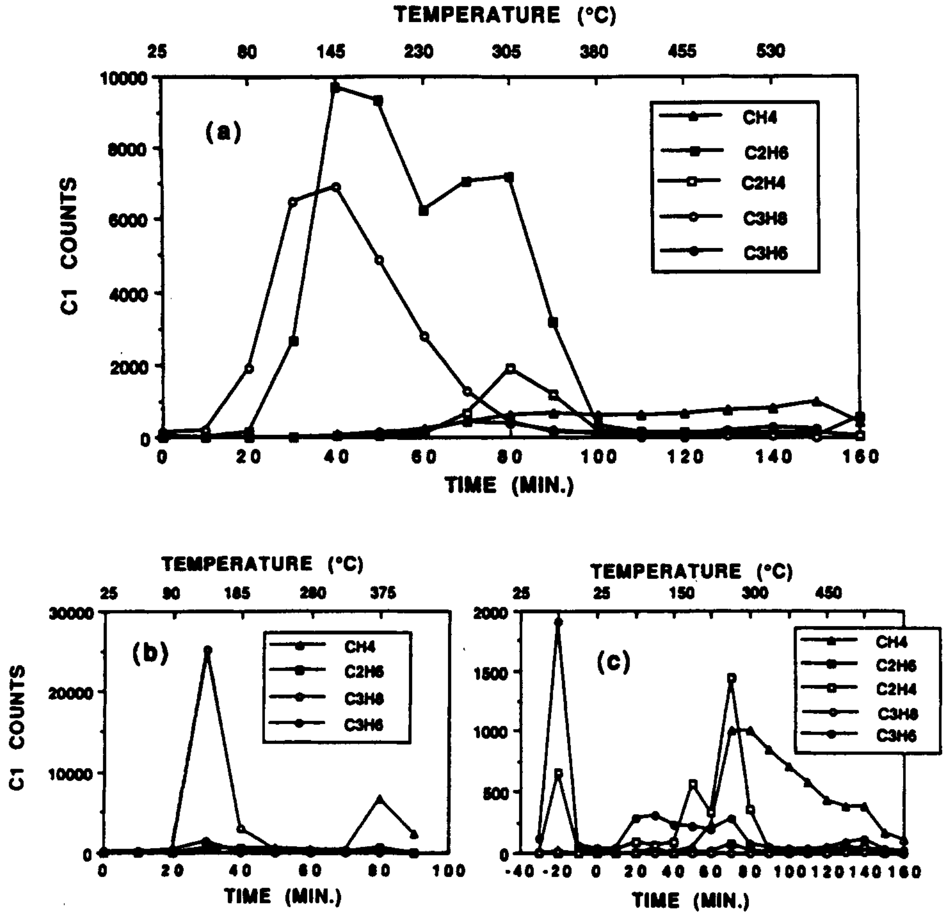

**Figure 1.** Temperature-programmed hydrogenolysis of $Mo_2(\eta^3\text{-}C_3H_5)_4$ in 6% $H_2$: (a) supported on Nissan Kagaku alumina, (b) pure compound, and (c) supported on Nissan Kagaku alumina and intentionally air-contaminated 30 min before heating.

samples were dried at 120 °C for 16 h and calcined at 500 °C for 16 h. Alumina pores were filled with aqueous $H_2(MoO_3C_2O_4)$ (Climax Molybdenum Co.) solutions of pH 1.5 or 6. Samples prepared with 1.5% Mo were dried at 120 °C for 3 h followed by calcination at 500 °C for 3 h.

LRS and UVDRS instruments and procedures were described previously.[45] $Mo/Al_2O_3$ samples supported on Ketjen and Nishio aluminas were calcined for 14 h at 480 °C and then for 3 h at 630 °C immediately before use to reduce background fluorescence. Samples prepared from Harshaw alumina were examined several months after calcination at 650 °C for 16 h.

## Results

**Temperature-Programmed Hydrogenolysis.** When heated in hydrogen, the allyl ligands of the molybdenum allyl surface compound were removed in a two-peak pattern, similar to that found by Iwasawa et al.[3] for this precursor and support. Ethane and propane first evolved near 170 °C, followed at 320 °C by ethane and ethylene (Figure 1a). Under identical ramp conditions the unsupported $Mo_2(\eta^3\text{-}C_3H_5)_4$ compound decomposed of 135 °C, producing primarily propane (Figure 1b). When the alumina-supported compound was intentionally contaminated with oxygen at room temperature, a large peak of propylene and ethylene was observed, and the supported compound, which had been dark green on this alumina, immediately became pale brown. When the sample was subsequently heated in 6% $H_2$, a different TPH pattern was observed and the residual hydrocarbons were removed as methane and ethylene (Figure 1c).

**Raman Spectra.** Raman analysis of $Mo^{6+}/Al_2O_3$ revealed, for samples examined under ambient conditions and in a hydrated state, spectra of crystalline $MoO_3$ and two surface molybdate species: isolated, tetrahedrally coordinated molybdate and polymeric, octahedrally coordinated molybdate. The dependence of surface molybdate structure on Mo content can be illustrated with the Raman spectra of samples prepared from AHM and Harshaw alumina (Figure 2). These samples were originally calcined at 650 °C and were examined several months after preparation. At 0.67% Mo, the spectrum displays bands at 918 and 315 cm$^{-1}$ with a shoulder at 847 cm$^{-1}$ (Figure 2d). As will be discussed below, these features are characteristic of isolated tetrahedrally coordinated surface molybdates. At 13.3% Mo (Figure 2a), the spectrum displays a strong band at 959 cm$^{-1}$, with a broad low-frequency shoulder, and two less intense bands at 360 and 220 cm$^{-1}$. These features are characteristic of octahedrally coordinated polymolybdate, as will be shown. As the Mo loading was increased from 0.67%, the high-frequency band shifted from 918 to 959 cm$^{-1}$. There was little change in the position of this band after the Mo content reached 6.7%. The band initially at 315 cm$^{-1}$ shifted to 360 cm$^{-1}$ with increasing Mo content (Figure

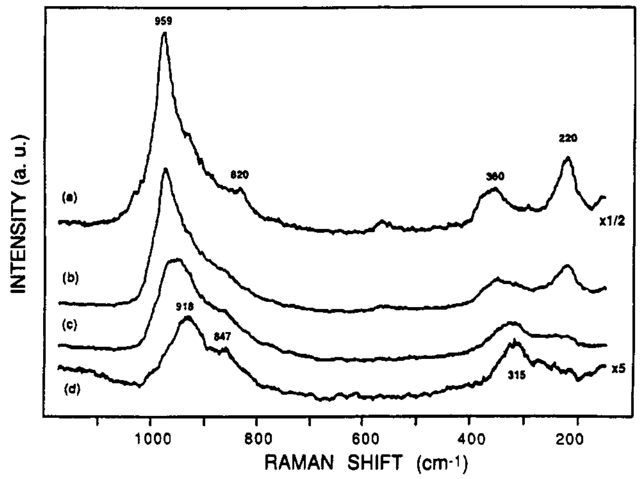

**Figure 2.** Raman spectra of $Mo^{6+}/Al_2O_3$ prepared from $(NH_4)_6Mo_7O_{24}\cdot 4H_2O$ and Harshaw alumina calcined at 650 °C: (a) 13.3% Mo, (b) 6.7% Mo, (c) 3.3% Mo, and (d) 0.67% Mo. Samples were air-exposed for several months before examining.

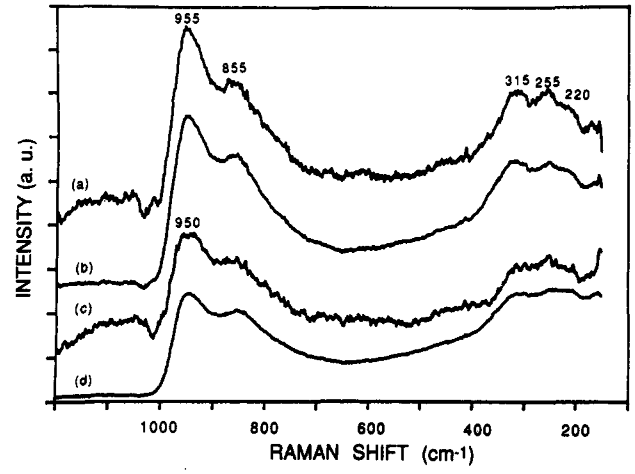

**Figure 3.** Raman spectra of (a) 1.6% $Mo^{6+}/Al_2O_3$ prepared from $Mo_2(\eta^3\text{-}C_3H_5)_4$ and Ketjen alumina, (b) 1.6% $Mo^{6+}/Al_2O_3$ prepared from $Mo_2(\eta^3\text{-}C_3H_5)_4$ and Nissan Kagaku alumina, (c) 1.0% $Mo^{6+}/Al_2O_3$ prepared from $Mo_2(\eta^3\text{-}C_3H_5)_4$ and Ketjen alumina, and (d) 1.0% $Mo^{6+}/Al_2O_3$ prepared from $Mo_2(\eta^3\text{-}C_3H_5)_4$ and Nissan Kagaku alumina. Samples were examined within 1 h of calcination at 630 °C.

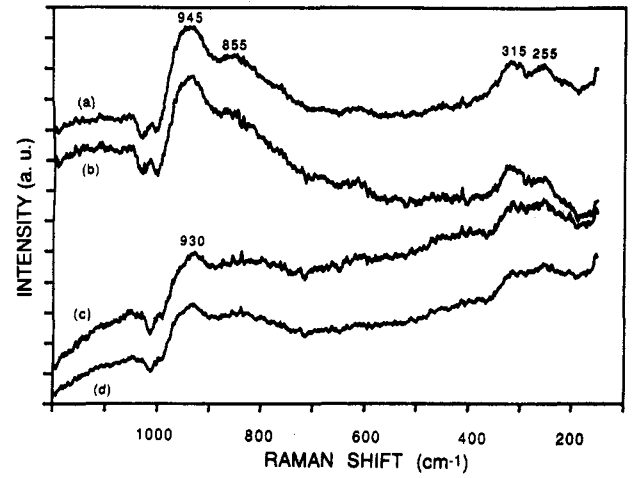

**Figure 4.** Raman spectra of (a) 1.5% $Mo^{6+}/Al_2O_3$ prepared from $H_2(MoO_3C_2O_4)\cdot 2H_2O$ and Ketjen alumina at pH 2, (b) 1.5% $Mo^{6+}/Al_2O_3$ prepared $H_2(MoO_3C_2O_4)\cdot 2H_2O$ and Ketjen alumina at pH 6, (c) 1.0% $Mo^{6+}/Al_2O_3$ prepared from $(NH_4)_6Mo_7O_{24}\cdot 4H_2O$ and Ketjen alumina at pH 6, and (d) 1.0% $Mo^{6+}/Al_2O_3$ prepared from $(NH_4)_6Mo_7O_{24}\cdot 4H_2O$ and Ketjen alumina at pH 9.1. Samples were examined within 1 h of calcination at 630 °C.

2a). At 6.7% Mo, the low-frequency shoulder, corresponding to the Mo–O–Mo bending mode, which can be observed at 0.67% Mo, became an intense band centered at 220 $cm^{-1}$ (Figure 2b). The Mo–O–Mo symmetric stretching mode of polymolybdate can be seen at 555 $cm^{-1}$ for the samples containing 6.7 and 13.3% Mo.[20] Bulk $MoO_3$ characterized by the Raman band at 820 $cm^{-1}$ [47] was present in the 13.3% Mo sample (Figure 2a).

The Raman spectra, recorded immediately after calcination, of samples prepared from $Mo_2(\eta^3\text{-}C_3H_5)_4$, $H_2(MoO_3C_2O_4)\cdot 2H_2O$, and AHM supported on Ketjen and Nishio aluminas were similar to the air-exposed, Harshaw-supported samples that contained similar Mo loadings. The most significant difference was the position of the high-frequency $\nu$(Mo–O) mode. Raman spectra of 1.6% $Mo/Al_2O_3$ prepared from $Mo_2(\eta^3\text{-}C_3H_5)_4$ supported on Ketjen and Nishio $\gamma$-aluminas displayed this band at 955 $cm^{-1}$ (Figure 3a,b). The position of this band decreased to 950 $cm^{-1}$ when the Mo content was lowered to 1.0% (Figure 3c,d). Spectra obtained from Ketjen alumina impregnated with $H_2(MoO_3C_2O_4)\cdot 2H_2O$ at both pH 1.5 and pH 6 were identical (Figure 4a,b), the high-frequency $\nu$(Mo–O) mode appearing at 945 $cm^{-1}$.

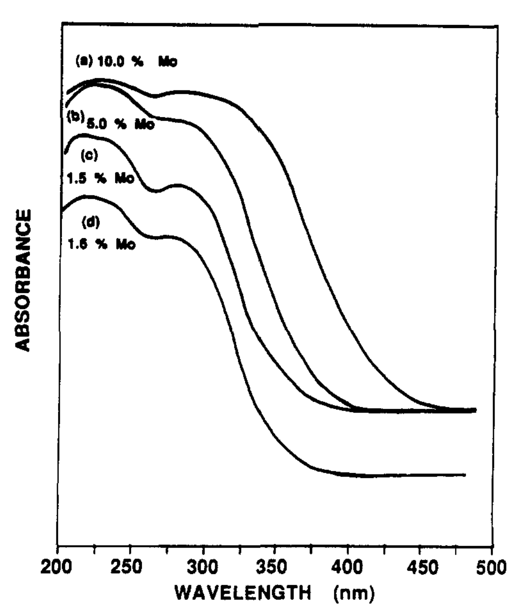

**Figure 5.** Ultraviolet–visible diffuse reflectance spectra of $Mo^{6+}$ supported on Ketjen alumina: (a) 10.0% Mo prepared from $(NH_4)_6Mo_7O_{24}\cdot 4H_2O$, (b) 5.0% Mo prepared from $(NH_4)_6Mo_7O_{24}\cdot 4H_2O$, (c) 1.5% Mo prepared from $(NH_4)_6Mo_7O_{24}\cdot 4H_2O$, and (d) 1.6% Mo prepared from $Mo_2(\eta^3\text{-}C_3H_5)_4$.

Samples prepared from AHM by equilibrium adsorption at pH 9.1 and by simple pore filling impregnation at pH 6 both exhibited high-frequency bands at 930 $cm^{-1}$ (Figure 4c,d). For Mo loadings of 1–3%, the $\nu$(Mo–O) mode decreased 15–20 $cm^{-1}$ when the same samples were examined 2 weeks later. The small band at 255 $cm^{-1}$ in the spectra presented in Figures 3 and 4 is due to a trace of $\theta$-alumina, which probably resulted from an alumina phase transition during calcination with Mo present.

**Ultraviolet–Visible Diffuse Reflectance Spectroscopy.** UVDRS spectra of $Mo/Al_2O_3$ all contain a strong broad band centered at 220–230 nm, common to both Mo($T_d$) and Mo($O_h$)[41,48] (Figure 5a–d). At low Mo levels a second broad band appeared at 280 nm. At higher Mo content this band broadened toward higher wavelengths. The UVDRS spectra of 1.5% $Mo/Al_2O_3$ prepared from AHM and $Mo_2(\eta^3\text{-}C_3H_5)_4$ are identical (Figure 5c,d). Calcination at 500 °C for 5 h had no effect on the UVDRS spectra of $Mo/Al_2O_3$; a similar observation was made by Rodrigo et al.[6]

## Discussion

The Raman spectra reported herein were recorded over $Mo^{6+}/Al_2O_3$ samples that were maintained in an ambient environment, following calcination. Recent in situ Raman studies[27,30,33,34,44] show that, under the ambient conditions employed, the surfaces of the oxide carrier are hydrated and the supported-surface oxides, in this case the surface molybdate species, are solvated by the water present on the surface. The discussion that follows is consistent with and reinforces the arguments presented in the preceding paper,[45] in which the case was made for the use of aqueous molybdate anions as models for the surface molybdate species. (A more general discussion of hydrated oxide structure can be found in ref 49.) The surface molybdate structures over alumina respond to the local aqueous environment of the surface, following calcination and exposure to ambient, and are not related to the precursor or the method of preparation.

The point of zero surface charge (PZSC) represents the pH at which the surface of an oxide is electrically neutral in an aqueous environment. The PZSC of quartz ($\alpha$-$SiO_2$) is 1–2, while that of alumina is typically 7–9.[50] The structure of the surface molybdate species is controlled by the PZSC of the hydrated surface. The PZSC changes from the zero-coverage limit as the

---

[47] Py, M. A.; Schmid, Ph. E.; Vallin, J. T. *Nuovo Cimento* **1977**, *38B*, 271.

[48] Fournier, M.; Louis, C.; Che, M.; Chaquin, P.; Masure, D. *J. Catal.* **1989**, *119*, 400.

[49] Deo, G.; Wachs, I. E. *J. Phys. Chem.* **1991**, *95*, 5889.

[50] Parks, G. A. *Chem. Rev.* **1965**, *65*, 177.

molybdenum oxide coverage changes because the molybdena ions modify the support oxide. Since molybdenum oxide is acidic in character, the PZSC of alumina is expected to decrease with increasing molybdena loading. In a separate study we have found the PZSC of Ketjen 000-1.5E alumina to decrease from 7.7 to 7.6, 7.2, 7.0, and 5.2 for Mo loadings of 0.1, 0.5, 1.0, and 5.0 wt %, respectively.[46] (Harshaw alumina had a PZSC of 8.0.) Changes in the PZSC with coverage of a second oxide layer have also been reported for vanadia on alumina and titania.[51]

A number of publications have appeared that detail the changes in the molybdenum ions with pH and concentration for aqueous solutions.[52-55] At pH above ca. pH 7, $MoO_4^{2-}(T_d)$ predominates, and below pH 6.8, the $Mo_7O_{24}^{6-}(O_h)$ polyanion forms. Below ca. pH 2.2, $Mo_8O_{26}^{4-}(O_h)$ forms. Both $MoO_4^{2-}$ and $Mo_7O_{24}^{6-}$ are present between pH 5 and 6.8.[52,53] The relative amount of each molybdenum anion is dependent on the pH and the total Mo concentration. We propose that at low $Mo^{6+}$ loadings tetrahedrally coordinated $MoO_4$ should predominate because the surface of alumina, when hydrated, has a PZSC near the zero-coverage limit of ca. 7–8. As the coverage increases and the PZSC decreases,[46] the octahedrally coordinated $Mo_7O_{24}$ polyanion should begin to form in response to both a lower PZSC and higher molybdena concentration. At sufficiently high coverage the $Mo_7O_{24}$ polyanion should predominate. These surface molybdate species are expected to form following calcination and exposure of the samples to ambient conditions, which hydrates the surface and hydrolyzes the structures that have been reported to form during in situ studies. The molybdate species should not be influenced by the precursor or method of preparation following the calcination step; the loading and PZSC of the hydrated surface should have the greatest influence on the species formed.

Most LRS studies of $Mo/Al_2O_3$ have detected five broad bands resulting from surface molybdate species at 975–920, 880–840, 360–330, 325–315, and 240–210 $cm^{-1}$. Many authors,[8,21,22,24,25,33] by analogy to the Raman spectrum of aqueous $Mo_7O_{24}^{6-}$, agree that an octahedrally coordinated polymolybdate species may be characterized by the broad bands at 950–975, 350–360, and 220 $cm^{-1}$, which are associated with the $\nu$(Mo–O), $\delta$(Mo–O), and Mo–O–Mo deformation modes, respectively. Comparison with the Raman spectra of $Mo_7O_{24}^{6-}$ and $Mo_8O_{26}^{4-}$, and with the literature just mentioned, leads to the conclusion that the Raman spectra of $Mo^{6+}/Al_2O_3$ at high weight loadings, 6.7 and 13.3% Mo (Figure 2a,b), are characteristic of octahedrally coordinated polymolybdate, most likely $Mo_7O_{24}$ because polymolybdates form discrete clusters.

The Raman band at 916–940[25,31,35] and 945 $cm^{-1}$,[33] which was accompanied by the $\delta$(Mo–O) mode at ca. 320 $cm^{-1}$, has been assigned by these authors to the $\nu_s$(Mo–O) mode of tetrahedrally coordinated surface molybdate species. Other groups have assigned bands at 950[8,23] and 968 $cm^{-1}$ [2] to a tetrahedral surface molybdate species but did not present spectra in region of the $\delta$(Mo–O) mode that can be used to support the assignment. At low weight loadings, 0.67–1.0% Mo, Raman spectra of air-exposed samples (such as Figure 2d) and of some samples recorded immediately after calcination (Figure 4c,d) exhibit Mo–O stretching modes from 918 to 930 $cm^{-1}$ and the Mo–O bending mode at ca. 320 $cm^{-1}$. The aqueous $MoO_4^{2-}$ anion,[56] as well as a number of other compounds containing $MoO_4$ groups, such as $CaMoO_4$,[57] displays intense Raman Mo–O bending modes near 320 $cm^{-1}$. It is therefore proposed that $Mo^{6+}/Al_2O_3$ samples containing 0.67–1% Mo consist primarily of tetrahedrally coordinated molybdenum oxide (Figures 2d and 4c,d). Some polymerization, however, is identified for these samples by the weak Mo–O–Mo bending mode at 220 $cm^{-1}$.

For intermediate loadings, 1–3.3 wt % Mo corresponding to 0.33–1.13 $Mo/nm^2$, both the tetrahedral and polymolybdate structures were formed when the samples were in the hydrated state. Tetrahedral and octahedral crystalline compounds have Mo–O stretching frequencies in the region 930–970 $cm^{-1}$;[58] and, while spectra of crystalline compounds are not appropriate reference compounds for hydrated, oxide-supported Mo, the coincident wavenumber position for tetrahedral and octahedral structures illustrates the problem of assigning structure solely on the position of the Mo–O stretch. The $\delta$(Mo–O) and $\delta$(Mo–O–Mo) modes must also be considered. Hardcastle and Wachs have shown that the Mo–O Raman stretching band changes in response to the distortion of the $MoO_6$ ($O_h$) or $MoO_4$ ($T_d$) unit. The shorter the terminal (or capping) Mo–O bond(s), the higher the frequency for the band position.[58] For $Mo/Al_2O_3$ this band position has been shown to be extremely sensitive to the extent of hydration. A good illustration of this can be found in ref 39 where the Mo–O band position for 13.3% $Mo/Al_2O_3$ is reported to shift from 952 $cm^{-1}$ for a hydrated sample to 1003 $cm^{-1}$ when dehydrated and examined in situ under a moisture-free environment. In this case,[44] complete dehydration was reasoned to transform the surface molybdena species from polymolybdate clusters to $MoO_6$ species. In a related in situ study the dehydrated spectra for 0.5, 3.3, 6.7, 10.0, and 13.3% $Mo/Al_2O_3$ were also found to have a band at ca. 1000 $cm^{-1}$; the Mo–O–Mo absorbance was absent for the 0.5 and 3.3 wt % samples but could be detected for higher loadings, suggesting isolated $MoO_6$ species at the lowest loadings and some type of Mo–O–Mo interaction between the $MoO_6$ units at the higher loadings.[59] More subtle changes, which may be associated with the amount of adsorbed water present for a hydrated sample, have been reported for samples examined in ambient. For example, Stencel et al.[27] reported that the $\nu$(Mo–O) frequencies of $Mo^{6+}/Al_2O_3$ samples examined 3 months after calcination were 10–20 $cm^{-1}$ lower than when examined only 3 days after calcination.

The alumina-supported, hydrated structures are interpreted to be similar to aqueous $Mo^{6+}$ structures with $MoO_4^{2-}$ and $Mo_7O_{24}^{6-}$ serving as the model structures in the limits of low and high loading, respectively. The $Mo_7O_{24}^{6-}$ aqueous polyanion has a $\nu$(Mo–O) stretch as 943 $cm^{-1}$, a $\delta$(Mo–O) mode at 362 $cm^{-1}$, and a $\delta$(Mo–O–Mo) mode at 219 $cm^{-1}$. The $MoO_4^{2-}$ aqueous anion has a $\nu$(Mo–O) stretch at 897 $cm^{-1}$ and a $\delta$(Mo–O) mode at 317 $cm^{-1}$.[53]

At intermediate Mo loadings, 1.0–3.3% Mo (Figures 2c, 3, and 4a,b), occurrence of the Mo–O bending frequency at 320 $cm^{-1}$ reflects tetrahedral Mo symmetry, but the $\nu$(Mo–O) frequency (944–955 $cm^{-1}$) is closer to that usually associated with octahedrally coordinated molybdenum. The spectra in Figures 3 and 4 were recorded immediately after calcination. Similar samples scanned after 2 weeks of air exposure experienced a decrease in Mo–O stretching frequency of 15 $cm^{-1}$, similar to the behavior reported earlier.[27] The $\delta$(Mo–O) mode for Mo($O_h$) at 370–360 $cm^{-1}$ and for Mo($T_d$) at 320 $cm^{-1}$ and the Mo($O_h$) $\delta$(Mo–O–Mo) mode at 220–210 $cm^{-1}$ were not observed by us to differ in freshly calcined or air-stabilized samples. Because of the sensitivity of the $\nu$(Mo–O) mode to moisture content for hydrated samples, the bending modes may be a more reliable indicator of molybdenum symmetry. The samples containing 1.0–3.3% Mo (Figures 2c, 3, and 4a,b), therefore, had a significant fraction of tetrahedrally coordinated surface molybdate as evidenced by the 320-$cm^{-1}$ mode, even though the Mo–O stretching modes occur at frequencies closer to those usually associated strictly with polymolybdate.

The Raman $\nu$(Mo–O) frequency of $Mo^{6+}/Al_2O_3$, recorded under ambient conditions by several researchers[8,20,22,24,25,27,31,32,35] and the work reported herein, was examined as a function of molybdenum surface concentration. Frequencies from 920 to 960

---

(51) Gil-Llambias, F. J.; Escudey, A. M.; Fierro, J. L. G.; Agudo, L. *J. Catal.* **1985**, *95*, 520.

(52) Luthra, N. P.; Cheng, W. C. *J. Catal.* **1987**, *107*, 154.

(53) Griffith, W. P.; Lesniak, P. J. B. *J. Chem. Soc. A* **1969**, 1066.

(54) Aveston, J.; Anacker, E. W.; Johnson, J. S. *Inorg. Chem.* **1969**, *3*, 735.

(55) Baes, C. F.; Mesmer, R. E. In *The Hydrolysis of Cation*; John Wiley & Sons: New York, 1976.

(56) Weinstock, N.; Schulze, H.; Muller, A. *J. Chem. Phys.* **1973**, *59*, 5063.

(57) Khanna, R. K.; Brower, W. S.; Guscott, B. R.; Lippincott, E. R. *J. Res. Natl. Bur. Stand., Sect. A* **1968**, *72*, 81.

(58) Hardcastle, F. D.; Wachs, I. E. *J. Raman Spectrosc.* **1990**, *21*, 683.

(59) Vuurman, M. A.; Wachs, I. E. In Situ Raman Spectroscopy of Supported Metal Oxides on Alumina. To be submitted for publication in *J. Phys. Chem.*

$cm^{-1}$ have been reported at ca. 1 Mo atom/$nm^2$, while at a concentration of 5 Mo atoms/$nm^2$, frequencies range from 950 to 975 $cm^{-1}$. In all cases the $\nu$(Mo–O) frequency increased with coverage for a given preparation method (e.g., see Figure 2). The scatter in the reported $\nu$(Mo–O) frequencies is probably due to the well-documented sensitivity of this vibrational mode to the degree of sample hydration, which is affected by the thermal history of the sample[27,30,33] and the laser power.[34] The increase of band position with coverage is consistent with a model that the structure of the supported Mo is controlled by the amount of Mo present and the PZSC of the hydrated support. In the case of $Mo^{6+}/Al_2O_3$ three stages can be identified.

In the first stage (<2 Mo atoms/$nm^2$), the polymolybdate species first begins to appear, along with the tetrahedral species, and increases in amount as the Mo content is increased. In this region, the Mo–O stretching freqeuncy increased dramatically with increasing Mo content while the low-frequency region of the spectra (Figure 2 and ref 20) remained dominated by the tetrahedral bending mode at 315–320 $cm^{-1}$. This behavior is illustrated in Figure 2c,d where the Mo–O stretching band increases from 918 to 944 $cm^{-1}$ while the Mo–O bending mode increases only slightly in frequency.

In the second stage (2–5 Mo atoms/$nm^2$), polymolybdate formation continues until an apparent monolayer limit is reached. The $\nu$(Mo–O) frequency does not increase as much as in the first stage, and the polymolybdate features, the Mo–O bend at 350–360 $cm^{-1}$ and the Mo–O–Mo deformation at 220 $cm^{-1}$, dominate the low-frequency portion of the spectra. In Figure 2, the low-frequency region is changed from nearly isolated $MoO_4$ tetrahedra (Figure 2c) to polymolybdate octahedra (Figure 2b). Once the low-frequency region assumes bands characteristic of polymolybdate, the Mo–O stretching frequency increases only from 956 to 959 $cm^{-1}$ (Figure 2a,b).

The designations of tetrahedrally and octahedrally coordinated molybdenum oxide species represent limiting models for the actual catalyst structures; most spectra contain features characteristic of both cases. A weak shoulder, due to Mo–O–Mo, appears at 220 $cm^{-1}$ in the spectrum of "isolated" tetrahedra (Figure 2d), and it is not possible to determine whether small amounts of tetrahedrally coordinated molybdenum contribute to the polymolybdate spectrum (Figure 2a).

Finally, at high Mo loadings, monolayer coverage of surface molybdates is exceeded and crystalline $MoO_3$ can be detected in the Raman spectra. (Figure 2a, 5.7 Mo atoms/$nm^2$, has the $MoO_3$ absorbance at 820 $cm^{-1}$.) A monolayer, assuming 17–20 Å$^2$/$MoO_3$ unit,[60] corresponds to 5 or 6 Mo atoms/$nm^2$, which is close to the number of Mo atoms in the heptamolybdate polyanion. This boundary attempts to define the onset of $MoO_3$ from many sets of spectra. There are, however, some exceptions to this boundary, such as the observation of $MoO_3$ at 2.3 Mo atoms/$nm^2$.[20] Apparently, the 2-h calcination time used for this[20] sample was insufficient for $MoO_3$, formed from excess local molybdenum concentrations, to decompose and wet the alumina surface. Also, $MoO_3$ was not detected for samples containing 4.9,[8] 5.2,[27] and 5.3 Mo atoms/$nm^2$,[24] probably because monolayer coverage had not yet been reached.

The $\nu$(Mo–O) frequencies for a series of samples prepared from $Mo_2(\eta^3\text{-}C_3H_5)_4$ and Nishio alumina and with loadings of 0.2–0.4 Mo atoms/$nm^2$ (Figure 3) are slightly higher than for similar loadings of samples prepared from $(NH_4)_6Mo_7O_{24}\cdot 4H_2O$ (Figure 2). The cause of these differences is not known. Apparently, a higher percentage of the Mo formed polymolybdate clusters from the $Mo_2(\eta^3\text{-}C_3H_5)_4$ precursor, as evidenced by the increasingly intense Mo–O–Mo deformation in these spectra, and this may contribute to the relatively high frequencies for the Mo–O stretching mode.

Molybdenum oxide dimers have been proposed to form from $Mo_2(\eta^3\text{-}C_3H_5)_4$ over alumina;[3] however, no Raman spectra have been presented for dimer structures. If dimers form, one might expect the $Mo_2O_7^{2-}$ anion to serve as a reference compound against which Raman spectra of supported Mo can be compared. The $Mo_2O_7^{2-}$ anion, made up from two corner-sharing $MoO_4$ tetrahedra, is found in crystalline $MgMo_2O_7$[61] and has been synthesized as a tetrabutylammonium salt.[62] The Raman spectrum of this ion, obtained from molten $K_2Mo_2O_7$,[63] displays a Mo–O symmetric stretch at 927 $cm^{-1}$ and a Mo–O bend at 335 $cm^{-1}$. The antisymmetric stretching and symmetric bending modes of the Mo–O–Mo linkage were observed at 883 and 196 $cm^{-1}$, respectively. Although these frequencies correlate well with those in Figures 3 and 4, the formation of molybdenum oxide dimers on oxide supports is very unlikely because the $Mo_2O_7^{2-}$ anion is stable only in the environments described above. The anion cannot be formed in aqueous environments,[62] double salts containing it decompose in water,[64] and the surfaces we examined were in a hydrated state.

With the interpretation of our Raman data, several important observations can be made about the $Mo/Al_2O_3$ system. First, the structure of calcined samples and the Raman spectra were only minimally dependent on the precursor. In line with the conclusions of Kasztelan et al.,[10] the samples prepared at high pH, from dilute AHM solutions, produced Raman spectra identical with those of samples prepared by pore filling of AHM solutions at their natural pH of 5–6 (Figure 4c,d). Calcined molybdenum oxalate samples prepared at pH 1.5 and 6, where initial adsorption is thought to occur through dimeric and monomeric molybdenum oxalate complexes, respectively, both produced the same Raman spectra. Spectra from samples prepared from $Mo_2(\eta^3\text{-}C_3H_5)_4$ on both Ketjen and Nishio aluminas were the same (Figure 3). At 1.0% Mo, the samples prepared from $Mo_2(\eta^3\text{-}C_3H_5)_4$ (Figure 3c,d) displayed a Mo–O stretching frequency 15 $cm^{-1}$ higher than the samples prepared from AHM (Figure 4c,d). This frequency difference is not thought to be associated with different structures. Iwasawa and Ogasawara[2] reported Raman bands at 968 and 960 $cm^{-1}$ for 1.5% Mo prepared from $Mo(\eta^3\text{-}C_3H_5)_4$ and AHM, respectively, which they associated with isolated tetrahedral Mo (968 $cm^{-1}$) and octahedral Mo (960 $cm^{-1}$). Samples we prepared from $H_2(MoO_3C_2O_4)\cdot 2H_2O$ also displayed higher $\nu$(Mo–O) frequencies than did samples prepared from AHM. Although there are some minor precursor-dependent variations in the spectra of Figures 3 and 4, these spectra are considered to represent surface molybdate species which are more similar than different. They all contain a mixture of surface tetrahedral and octahedral molybdates. There is no evidence for the preferential formation of Mo dimers or cation pairs from preparation with $H_2(MoO_3C_2O_4)\cdot 2H_2O$ at low pH or with $Mo_2(\eta^3\text{-}C_3H_5)_4$.

More significant differences in structure are seen to stem from molybdenum content. The Mo–O stretching frequency of samples prepared from $Mo_2(\eta^3\text{-}C_3H_5)_4$ and Nishio alumina increased from 940 $cm^{-1}$ at 0.7% Mo to 955 $cm^{-1}$ at 1.6% Mo. From our discussion above, these samples contain a mixture of $MoO_4$ tetrahedra and polymolybdate octahedra. The degree of polymerization rapidly increases with Mo loading because Mo is causing the alumina support to have a lower PZSC and because at the lower PZSC polymolybdate formation is concentration dependent. This casts doubt on the notion that the structure of $Mo^{6+}/Al_2O_3$ prepared from allylic precursors is identical over a range of weight loadings, 0.2–2% Mo.[4] It is concluded that the final structure of fully oxidized $Mo/Al_2O_3$ is more dependent on the weight loading than the Mo precursor.

The interpretation and limitations of UVDRS of supported $Mo^{6+}$ have been reviewed.[45,48] The UVDRS data allow a direct comparison with Raman results for the same samples. This comparison permits us to suggest UV absorbance assignments for $Mo/Al_2O_3$. The UV spectra of $Mo^{6+}/Al_2O_3$ (Figure 5) are similar

---

(60) Fransen, T.; Van Berge, P. C.; Mars, P. In *Preparation of Catalysts II*; Elsevier: Amsterdam, 1976; p 45.

(61) Stadnicka, K.; Haber, J.; Kozlowski, R. *Acta Crystallogr.* **1977**, *B33*, 3859.

(62) Day, V. W.; Frerich, M. F.; Klemperer, W. G.; Shum, W. *J. Am. Chem. Soc.* **1977**, *99*, 6146.

(63) Becher, H. J. *J. Chem. Res. (M)* **1980**, 1053.

(64) Becher, H. J.; Brockmeyer, H.-J.; Prigge, U. *J. Chem. Res. (M)* **1978**, 1670.

to those reported for $Mo^{6+}/SiO_2$.[45] Both sets of spectra contain a peak at 230 nm, common to reference compounds of tetrahedrally and octahedrally coordinated molybdenum.[41,48] The 280-nm absorbance for $Mo^{6+}/SiO_2$ samples, containing 0.5–2% Mo, was attributed to octahedrally coordinated $Mo^{6+}$ because Raman results demonstrated that this was the only type of molybdenum on the surface. The Raman spectrum of 1.5% $Mo^{6+}/Al_2O_3$ indicated that both tetrahedrally and octahedrally coordinated molybdenum were present; therefore, consistent with the assignment over silica, the 280-nm absorbance is associated with $Mo(O_h)$. Also, as established by Raman spectroscopy, for high Mo content (5–10% Mo), the increased absorption at 320–350 nm is associated with $Mo(O_h)$. Finally, Raman spectroscopy demonstrated that identical structures of $Mo^{6+}/Al_2O_3$ were prepared from both $Mo_2(\eta^3\text{-}C_3H_5)_4$ and AHM. The absorbance maximum at 280 nm for samples prepared from $Mo_2(\eta^3\text{-}C_3H_5)_4$ corresponds exactly with that in the UVDRS spectrum reported by Iwasawa and Ogasawara[2] for $Mo^{6+}/Al_2O_3$ prepared from $Mo(\eta^3\text{-}C_3H_5)_4$. This observation, coupled with similar Raman results for Iwasawa and Ogasawara samples made from $Mo(\eta^3\text{-}C_3H_5)_4$ and AHM, suggests that similar structures were formed by the two different research groups using either $Mo_2(\eta^3\text{-}C_3H_5)_4$, $Mo(\eta^3\text{-}C_3H_5)_4$, or AHM.

**Factors Controlling Surface Molybdate Structure.** As demonstrated above, the structure of supported molybdenum oxide is more dependent on inherent acid–base interactions than on preparation procedure. Other workers have concluded that the structure of supported molybdenum oxide is independent of the preparation procedure and dependent on the nature of the support.[65-67]

The use of allylmolybdenum compounds was reported[4] to produce stable isolated surface species irrespective of the above acid–base considerations on silica and alumina. We have been unable to differentiate the structure of fully oxidized, allyl-derived surface species with LRS and UVDRS from those prepared from other precursors for samples on silica, alumina, and magnesia. The TPH results for $Mo_2(\eta^3\text{-}C_3H_5)_4/Al_2O_3$ illustrate that the initial fixation of allylmolybdenum compounds occurred in a fashion similar to that reported by Iwasawa et al.[3] Oxygen contamination and failure of the allyl compounds to bond to the support, two errors which could have explained the discrepancy, can therefore be ruled out for the samples used in our work. It appears that calcination and exposure to ambient causes surface bound molybdenum cations, which may have initially been strictly "monomeric" or "dimeric", to assume structures that depend on the PZSC of the hydrated support: molybdenum polymerizes to discrete octahedral clusters on silica[45] and, depending on the Mo loading, forms isolated $MoO_4$ groups or polymolybdate on alumina.

## Conclusions

1. The structure of surface molybdates following calcination and rehydration by exposure to ambient for $Mo^{6+}/Al_2O_3$ samples is virtually independent of the molybdenum precursor. Rather, the surface molybdate structure is dependent on the inherent acid–base properties of the molybdena/alumina system.
2. At very low Mo loadings (<1 Mo atom/nm$^2$) $MoO_4$ tetrahedra are formed on alumina. As the Mo content is increased, the PZSC of the alumina decreases and discrete polymeric molybdates are formed. $MoO_3$ is formed after the polymolybdate monolayer has been reached (5–6 Mo atoms/nm$^2$).

*Acknowledgment.* This work was supported by the Robert A. Welch Foundation and the U.S. Department of Energy, Office of Basic Energy Sciences (C.C.W. and J.G.E.), and by the Texaco Philanthropic Foundation (F.D.H.). We acknowledge Prof. Y. Iwasawa for supplying alumina supports.

**Registry No.** Molybdenum oxide, 1313-27-5.

---

(65) Stampfl, S. R.; Chen, Y.; Dumesic, J. A.; Niu, C.; Hill, C. G., Jr. *J. Catal.* **1987**, *105*, 445.
(66) Leyrer, J.; Vielhaber, B.; Zaki, M. I.; Zhuang, S.; Weitkamp, J.; Knozinger, H. *Mater. Chem. Phys.* **1985**, *13*, 301.
(67) Hayden, T. F.; Dumesic, J. A. *J. Catal.* **1987**, *103*, 366.

---

# Absorption Band Shape Analysis for Photoinduced Intermolecular Electron Transfer in Solution. Application to a New Near-Infrared Transition between Free Hexacyanoferrate(II) and Hexacyanoferrate(III)

**Dimitrij E. Khoshtariya,[†] Anna M. Kjaer,[‡] Tamaz A. Marsagishvili,[†] and Jens Ulstrup*,[‡]**

*Institute of Inorganic Chemistry and Electrochemistry of the Georgian Academy of Sciences, Jikiya 7, 380086 Tbilisi, USSR, and Chemistry Department A, Building 207, The Technical University of Denmark, 2800 Lyngby, Denmark* *(Received: October 12, 1990)*

A mixture of high concentrations of $[Fe(CN)_6]^{3-}$ and $[Fe(CN)_6]^{4-}$ in water and $D_2O$ exhibits a weak absorption band at 800 nm under conditions where binuclear mixed-valence complexes or hydration products cannot be detected. At constant cation concentration the band follows the Lambert–Beer law with respect to both components. The absorption increases on alkali halide addition, with small but notable variations along the alkali-metal series, but decreases with increasing temperature. It is suggested that this band is caused by photoinduced electron transfer in ion-paired outer-sphere mixed-valence configurations. Band shape analysis shows that extensive solvent and ion-pair reorganization occurs on electron transfer. From the band shape parameters it is concluded that the corresponding thermal process is close to the adiabatic limit. Rate constants calculated from the optical parameters are higher than reported values probably due to inhomogeneous band broadening.

## 1. Introduction

Close relations between radiationless electronic relaxation and optical absorption or emission have been recognized since the earliest theoretical approaches to electronic processes in solids and molecules.[1-5] Such correlations provide links between the rate constant or activation energy of a thermal transition in a given

---

* Address correspondence to this author.
[†] Georgian Academy of Sciences.
[‡] The Technical University of Denmark.

(1) Huang, K.; Rhys, A. *Proc. R. Soc. A* **1951**, *204*, 406.
(2) Lax, M. *J. Chem. Phys.* **1952**, *20*, 1752.
(3) Kubo, R. *Phys. Rev.* **1952**, *86*, 929.
(4) Pekar, S. I. *Untersuchungen über die Elektronentheorie der Kristalle*; Akademie Verlag: Berlin, 1954.
(5) Kubo, R.; Toyozawa, Y. *Prog. Theor. Phys.* **1955**, *13*, 161.

0022-3654/91/2095-8797$02.50/0